Acta Crystallographica Section C
Crystal Structure Communications
ISSN 0108-2701

The first 3′:5′-cyclic nucleotide–amino acid complex: L-His–cIMP[1]

Katarzyna Ślepokura

Faculty of Chemistry, University of Wrocław, 14 Joliot-Curie St, 50-383 Wrocław, Poland
Correspondence e-mail: katarzyna.slepokura@chem.uni.wroc.pl

Received 1 May 2012
Accepted 2 July 2012
Online 13 July 2012

In the crystal structure of the L-His–cIMP complex, *i.e.* L-histidinium inosine 3′:5′-cyclic phosphate [systematic name: 5-(2-amino-2-carboxyethyl)-1*H*-imidazol-3-ium 7-hydroxy-2-oxo-6-(6-oxo-6,9-dihydro-1*H*-purin-9-yl)-4a,6,7,7a-tetrahydro-4*H*-1,3,5,2λ^5-furo[3,2-*d*][1,3,2λ^5]dioxaphosphinin-2-olate], $C_6H_{10}N_3O_2^+\cdot C_{10}H_{10}N_4O_7P^-$, the Hoogsteen edge of the hypoxanthine (Hyp) base of cIMP and the Hyp face are engaged in specific amino acid–nucleotide (His···cIMP) recognition, *i.e.* by abutting edge-to-edge and by π–π stacking, respectively. The Watson–Crick edge of Hyp and the cIMP phosphate group play a role in nonspecific His···cIMP contacts. The interactions between the cIMP anions (*anti*/C3′–*endo*/*trans*–*gauche*/chair conformers) are realized mainly between riboses and phosphate groups. The results for this L-His–cIMP complex, compared with those for the previously reported solvated L-His–IMP crystal structure, indicate a different nature of amino acid–nucleotide recognition and interactions upon the 3′:5′-cyclization of the nucleotide phosphate group.

Comment

High-resolution crystal structures of amino acid–nucleotide complexes can serve as model systems to investigate protein–nucleic acid interactions and their manner of recognition. Nucleic acid-binding proteins discriminate between potential binding sites based on their sequence or structure or a combination of both. The forces involved in noncovalent protein–nucleotide/nucleic acid complex formation are relatively weak (hydrogen bonds, hydrophobic interactions, and π–π stacking between the base and aromatic side chain), but still crucial for the stability of the complex, and the overall affinity results from the sum of many interactions. Electrostatics, hydrophobic interactions and polar contacts involving direct or water-mediated hydrogen bonds are all evident and widespread (Rice & Correll, 2008).

In DNA–protein complexes, histidine has been shown to prefer interactions with guanine (Luscombe *et al.*, 2001), which is a 2-amino derivative of hypoxanthine and thus has the same Hoogsteen edge crucial for protein–DNA recognition. The nucleotide Hoogsteen edge, with its unique functional groups (hydrogen-bond donors and acceptors) exposed in the major groove, is associated with the main specifity of protein–B-DNA complexes. This is distinct from protein–RNA and protein–nucleotide recognition, in which the different edges of a base may play a similar role in protein binding, *viz.* the Watson–Crick edge, the Hoogsteen edge and the sugar edge (Leontis & Westhof, 2001).

The only examples of coordinating-metal-free complexes of amino acid/oligopeptide–nucleotide deposited so far in the Cambridge Structural Database (CSD, Version 5.33; Allen, 2002) are three isomorphous complexes of IMP (inosine 5′-monophosphate) with L-Ser (CSD refcode ZUWQEN; Mukhopadhyay *et al.*, 1995), L-Glu (QUSMIA; Bhattacharya *et al.*, 2000) and L-Gln (LIRQUY; Bera *et al.*, 1999), two complexes of N7-methylguanosine 5′-monophosphate (m^7GMP) with L-Phe and Trp–Glu [DUMJEA10 (Ishida *et al.*, 1988) and SEKXIP10 (Ishida *et al.*, 1991), respectively], and, most recently, isomorphous L-His–IMP·MeOH·H_2O (TUVZIU; Ślepokura & Petrus, 2010) and L-His–IMP·2.5H_2O (Ślepokura & Makarewicz, 2012). No crystal data on cyclic nucleotide–amino acid complexes are available to date. The analysis of structural details is difficult in the first four of the above-mentioned structures, mainly due to the lack of at least some of the H atoms and therefore incorrect ionization states. In addition, the crystal structure of the highly hydrated IMP–Ser/Glu/Gln complexes is dominated by IMP–IMP interactions and no direct specific nucleobase–amino acid side-chain interactions are observed.

Therefore, the synthesis and structural analysis of the title L-His–cIMP complex, (I), which reveals both specific and nonspecific interactions of L-histidine (His) with inosine 3′:5′-cyclic monophosphate (cIMP), have been undertaken. The conformation and binding mode of cIMP are compared with those found in the solvated L-His–IMP complexes and the other amino acid–IMP complexes deposited in the CSD, as well as with cIMP crystal structures reported to date, *viz.* cIMP·H_2O (BEPRAP; Sundaralingam *et al.*, 1982) and [Cu(cIMP)(phenanthroline)$(H_2O)_2$]$NO_3\cdot 2H_2O$ (CATTEW; Sheldrick, 1983).

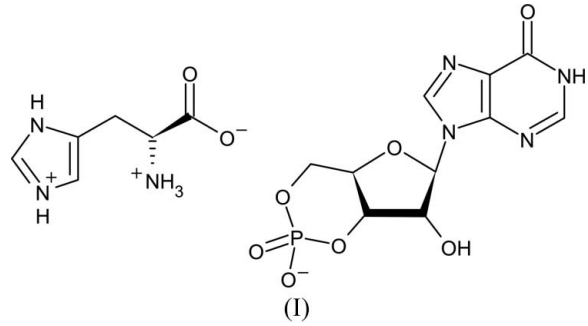

(I)

The asymmetric unit of (I) consists of a cIMP monoanion and a His cation, as shown in Fig. 1. Analogous to IMP in two isomorphous solvated L-His–IMP complexes, the cIMP nucleotide in (I) adopts a typical *anti* conformation about the

[1] Dedicated to Professor Tadeusz Lis on the occasion of his 65th birthday.

 doi:10.1107/S0108270112030041 © 2012 International Union of Crystallography

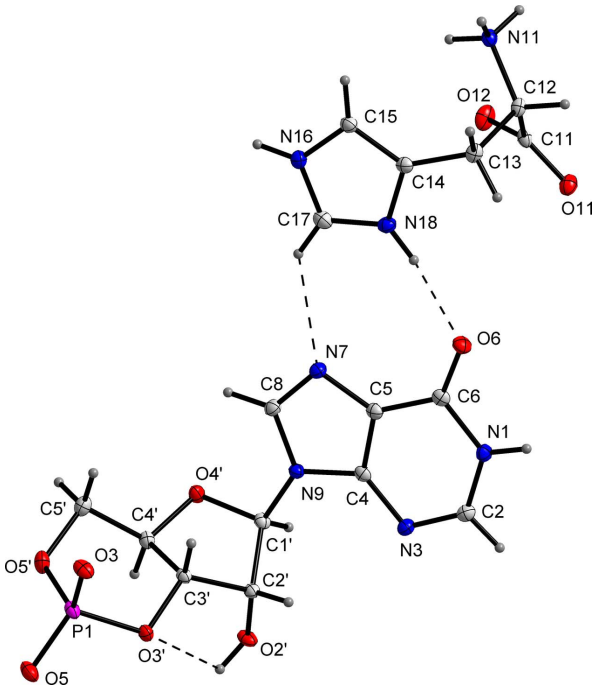

Figure 1
Views of the His cation and cIMP anion of (I), showing the atom-numbering schemes and the symmetry-independent N—H···O and C—H···N hydrogen bonds (dashed lines). The intramolecular O2′—H2′···O3′ contact is also shown. Displacement ellipsoids are drawn at the 50% probability level.

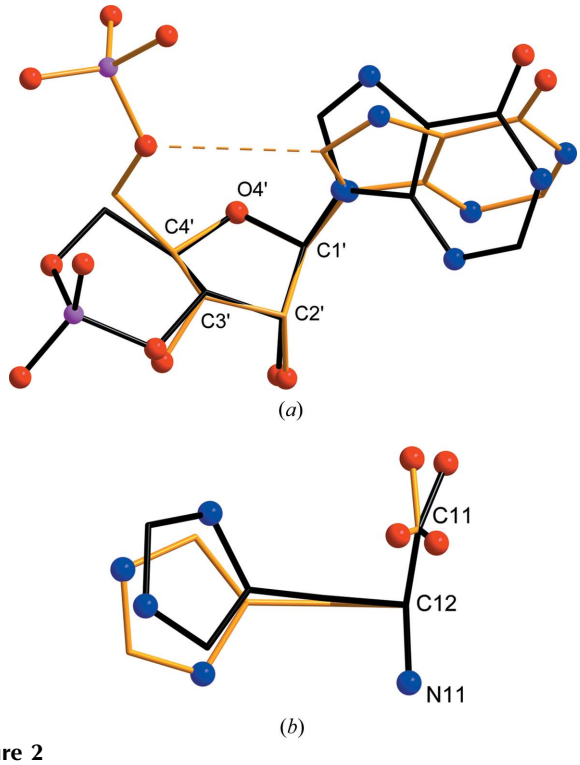

Figure 2
Comparison of the conformations of (*a*) the cIMP/IMP anions and (*b*) the His cations in L-His–cIMP (black; this work) and L-His–IMP·MeOH·H_2O (grey) (Ślepokura & Petrus, 2010; light orange in the electronic version of the paper). The common reference points are the labelled atoms. In IMP, the relative orientation of the hypoxanthine (Hyp) base and ester atom O5′ is stabilized by an intramolecular C8—H8···O5′ hydrogen bond (dashed line).

N-glycosidic C1′—N9 bond, although with a χ_{CN} O4′—C1′—N9—C4 torsion angle of −174.66 (12)°, which is uncommon [compared with −139.2 (5) and −138.5 (3)° observed in IMP in its complexes]. As shown in Fig. 2, the orientation of the Hyp base relative to the ribose ring in IMP and cIMP in their complexes with L-His is the main difference in the structures of these analogous nucleotides, despite the same formal *anti* glycosyl conformation.

Analogous to IMP in the solvated L-His–IMP complexes, the cIMP nucleotide in (I) is puckered in an envelope C3′-*endo* (^3E) manner, which is confirmed by the pseudorotation parameters (Rao *et al.*, 1981) P = 14.7 (1)° and τ_m = 46.5 (1)°, and the Cremer & Pople (1975) puckering parameters q_2 = 0.4561 (15) Å and φ_2 = 283.22 (17)°. It is worth mentioning that the ^3E conformation is one of two typically observed in free IMP and other free and protein-bound nucleotides (Allen, 2002; Moodie & Thornton, 1993), and was also observed in the solvated L-His–IMP complexes, but not in the other previously reported amino acid–nucleotide (both IMP and m^{7}GMP) complexes, in which C2′-*endo* (^2E) puckering is the most common. However, the ribose in the only crystal structures of cIMP reported so far, *viz.* cIMP·H_2O (BEPRAP; Sundaralingam *et al.*, 1982) and [Cu(cIMP)(phenanthroline)$(H_2O)_2$]NO_3·$2H_2O$ (CATTEW; Sheldrick, 1983), is found in a different puckering conformation, *i.e.* C3′-*endo*/C4′-*exo* ($^3T_4$). The ribose in protein-bound IMP does not reveal any conformational preference either.

The chair (*C*) conformation of the six-membered O/P/O/C/C/C 1,3,2-dioxaphosphorinane ring of the cIMP anion is significantly flattened at the P atom. This deformation of the ring towards an envelope (*E*) is reflected in the values of the dihedral angles between the least-squares plane through the four central atoms of the ring (O3′/O5′/C3′/C5′) and the O3′/P1/O5′ and C3′/C4′/C5′ planes [φ_1 = 44.5 (1)° and φ_2 = 59.4 (1)°; $\varphi_2 - \varphi_1$ = 14.9 (2)°], as well as in the Cremer–Pople puckering parameters: Q = 0.5959 (13) Å, θ = 172.88 (12)° and φ = 346.0 (11)°. It has been shown that, in small six-membered cyclic phosphates, the extent of *C*→*E* deformation is related to protonation or esterification of the cyclic phosphate group (Ślepokura & Lis, 2004; Ślepokura, 2008; Ślepokura & Mitaszewska, 2011). It is convenient to use the values of $|\varphi_2 - \varphi_1|$ (defined as the dihedral angles between the O—P—O and C—C—C planes, respectively) for a quantitative description of ring flattening. In small cyclic phosphates, the $|\varphi_2 - \varphi_1|$ values amount to several degrees for compounds with an ionized phosphate group, and to more than 12° for acidic or esterified molecules. However, this general rule seems not to be true in the cIMP anion of (I) presented here, in which $\varphi_2 - \varphi_1$ = 14.9 (2)°, nor in other cIMP anions reported to date ($\varphi_2 - \varphi_1$ = 18.2 and 14.8° for BEPRAP and CATTEW, respectively), nor in the other 3′:5′-cyclic nucleotides deposited in the CSD, in which $\varphi_2 - \varphi_1$ ranges from 10.9 to 20.9° (Allen, 2002).

Selected geometric parameters for (I), given in Table 1, indicate the deformation of the phosphate group from the

ideal tetrahedral shape, which is seen particularly in the endocyclic O3′—P1—O5′ and exocyclic O3—P1—O5 bond angles, which are, respectively, the smallest [103.48 (6)°] and the largest [117.75 (6)°]. These values of the endo- and exocyclic O—P—O angles correlate with the respective P—O bond lengths. In (I), as in other ionized six-membered cyclic phosphates (Ślepokura, 2008; Ślepokura & Mitaszewska, 2011), the P—O_{endo} bonds are all approximately 1.6 Å, and roughly 0.1 Å longer than the P—O_{exo} bonds.

The L-His cation in its complexes with both IMP and cIMP has the carboxy group deprotonated, and amino atom N11 and imidazole atom N16 (N^{ε}) protonated. As seen in Fig. 2(*a*), the His conformation is different. In both cases, the planes defined by the imidazolium ring and by the backbone NH_3^+—$C^{\alpha}12$—COO^- fragment are both approximately perpendicular to the $C^{\alpha}12$—$C^{\beta}13$—$C^{\gamma}14$ plane, which is reflected in the interplanar angles of 78.4 (1) and 87.6 (1)°, respectively, in (I), compared with 86.8 (4)/87.7 (4)° and 88.4 (2)/88.3 (2)° in two solvated L-His–IMP complexes (Ślepokura & Petrus, 2010; Ślepokura & Makarewicz, 2012). The location of protonated atoms N11 and N18 (N^{δ}) on different sides of the His cation in (I) differentiates it from His in complexes with IMP, and plays a role in the His···cIMP and His···IMP interactions, as will be discussed below. As shown in Fig. 2, and confirmed by the pseudotorsion angles N11—$C^{\alpha}12$—$C^{\gamma}14$—$C^{\delta}15$ of 2.7 (1)° [for His in (I)] and N11—$C^{\alpha}12$—$C^{\gamma}14$—$N^{\delta}18$ of −11.2 (1) and −10.6 (3)° (for His in IMP complexes), in L-His–cIMP the carboxylate (COO^-) group and the protonated N18 atom (N^{δ}) are located on the same side of the His cation, whereas in the solvated L-His–IMP complexes, protonated atoms N11 (NH_3^+) and N18 (N^{δ}) are on the same side of the His cation.

All the differences noted above in the chemical nature and structure of the components of the His–IMP and His–cIMP complexes translate into the nature of the interactions between His cations (His···His) and between nucleotide anions (cIMP···cIMP) and the most interesting and crucial to the amino acid–nucleotide recognition process, *i.e.* the His···cIMP contacts. As shown in Fig. 3, both His···His and cIMP···cIMP interactions arrange adjacent His cations or cIMP anions into infinite ribbons running down the *a* axis. The overall architecture of the His ribbon in (I) is similar to that in the solvated L-His–IMP complexes: each His cation is joined to four adjacent cations (related by a direct *a*-axis translation and a 2_1 symmetry operation) *via* a network of bifurcated N—H···O hydrogen bonds of a salt-bridge type, which are, however, much more compact than in His–IMP complexes (Fig. 3*a* and Table 2). As in His–IMP complexes, the imidazolium rings, which are located outside the ribbon, are exposed to specific amino acid–nucleotide interactions (Fig. 3*b*).

In contrast, the interactions between the cIMP anions in (I) are much less numerous than the IMP···IMP contacts in solvated His–IMP complexes. In (I), a direct *a*-axis translation generates infinite ribbons of cIMP anions *via* O—H···O interactions linking the ribosyl O2′—H2′ group with atom O3 of an adjacent cyclic phosphate group, and *via* C—H···O contacts linking the same hydroxy group with an adjacent

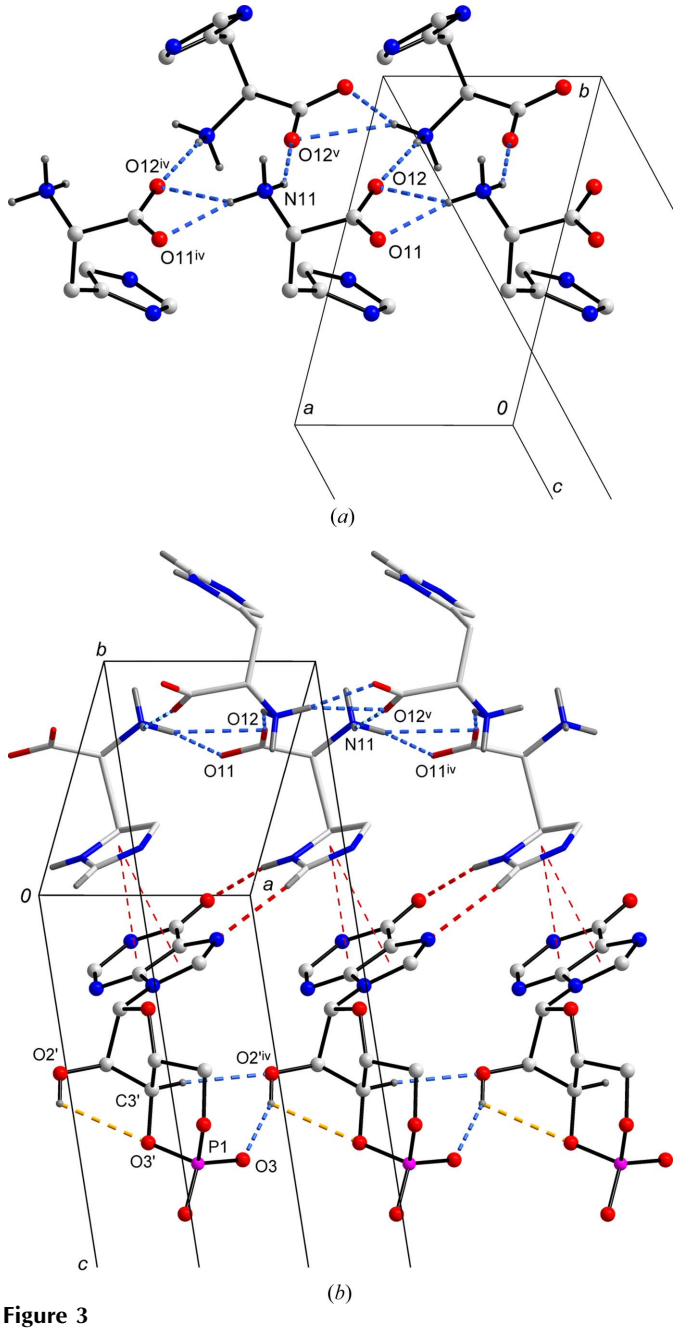

Figure 3
(*a*) The ribbon of His cations running down the *a* axis and (*b*) the specific His···cIMP edge-to-edge hydrogen bonds (thick dashed lines; red in the electronic version of the paper) and π–π stacking (thin dashed lines; red) with the cIMP ribbon. Intermolecular His···His and cIMP···cIMP interactions are shown as dashed lines (blue). H atoms not involved in hydrogen bonds have been omitted for clarity. [Symmetry codes: (iv) $x+1$, y, z; (v) $x+\frac{1}{2}$, $-y+\frac{3}{2}$, $-z$.]

ribosyl C atom (Fig. 3*b*). Notably, the hypoxanthine bases in (I) are not involved in the cIMP···cIMP contacts, and therefore may be used more efficiently for His–cIMP recognition. In addition, the monoionized cyclic phosphate group in (I) has no H atom, which excludes the possibility of phosphate–phosphate interactions. All these observations result in significant differences in mutual orientation and internucleotide interactions between IMP and its cyclic analogue,

cIMP in (I). It is worth mentioning that internucleotide contacts seem to predominate in the crystal structures of previously reported nucleotide–amino acid complexes. They are realised mainly *via* sugar–phosphate interactions (all but His–IMP) and contacts involving the base: sugar–base, like O2′···N3(Hyp) in His–IMP complexes, and base–phosphate, like N1(Hyp)···O_P in three other IMP complexes. In Phe–m^7GMP and solvated His–IMP complexes, additional phosphate–phosphate interactions also exist. Against this background, the internucleotide interactions in (I), with only sugar–phosphate contacts present, appear to be very simple.

In both the His–cIMP, (I), and His–IMP crystal complexes, the nucleotide Hoogsteen edge, commonly used in protein–nucleic acid recognition, is also involved in amino acid–nucleotide (His···cIMP and His···IMP) interactions. As shown in Figs. 1 and 3(*b*), in (I), the histidine side chain–Hyp base recognition is realised *via* specific edge-to-edge hydrogen bonds utilizing both Hyp Hoogsteen atoms N7 and O6, *i.e.* N^{δ}18–H18···O6(Hyp) and C^{ε}17–H17···N7(Hyp) (Table 2), as well as *via* π–π stacking of the cation···π type [centroid–centroid distances of 3.409 (2) and 3.438 (2) Å, respectively, for *Cg*(His)···*Cg*(Hyp-six-membered) and *Cg*(His)···*Cg*-(Hyp-five-membered) involving the Hyp anion at ($x+1$, y, z), with an interplanar spacing of 3.22 (1) Å; Fig. 3*b*]. In the isomorphous His–IMP complexes, interionic C^{δ}15—H15···O6(Hyp) and N^{ε}16—H16···N7(Hyp) interactions are found. Different His···Hoogsteen(Hyp) hydrogen bonds in His–cIMP and His–IMP complexes are accompanied by different conformations of the His cation (discussed above) and thus different orientations of the imidazolium ring relative to the nucleotide base. However, in each case, the orientation is retained such that the interactions of the δ and ε positions of the His cation with, respectively, atoms O6(Hyp) and N7(Hyp) of the nucleotide anion are achieved.

The specific nucleotide–amino acid interactions involving the base Hoogsteen edge are crucial in the recognition process. Direct amino acid side-chain–Hyp interactions were not observed in the other IMP–amino acid complexes, except for His–IMP, but they may be analysed in macromolecular protein–IMP complexes [see Ślepokura & Petrus (2010) for examples]. However, it is also known that, in protein–IMP complexes, the Watson–Crick edge is also involved in nucleotide–amino acid interactions, *e.g.* N1(Hyp)···amino acid side-chain interactions are commonly observed. As shown in Fig. 4, in (I), each cIMP anion utilizes the base Watson–Crick edge to form nonspecific N—H···O and C—H···O His···cIMP interactions, linking the Hyp atom N1 to the carboxylate group of the adjacent His cation, and Hyp atom O6 to the C12—H12 group of the same His cation. In this way, two different $R_2^2(8)$ rings (Bernstein *et al.*, 1995) are generated for each Hyp base with the participation of two different His cations. In contrast, the Watson–Crick edge of IMP in His–IMP complexes is involved in solvent-mediated IMP···MeOH/H_2O···IMP contacts, and therefore does not bind His at all.

As seen from a number of contacts involving the cIMP nucleotide anionic cyclic phosphate group in (I), it may be

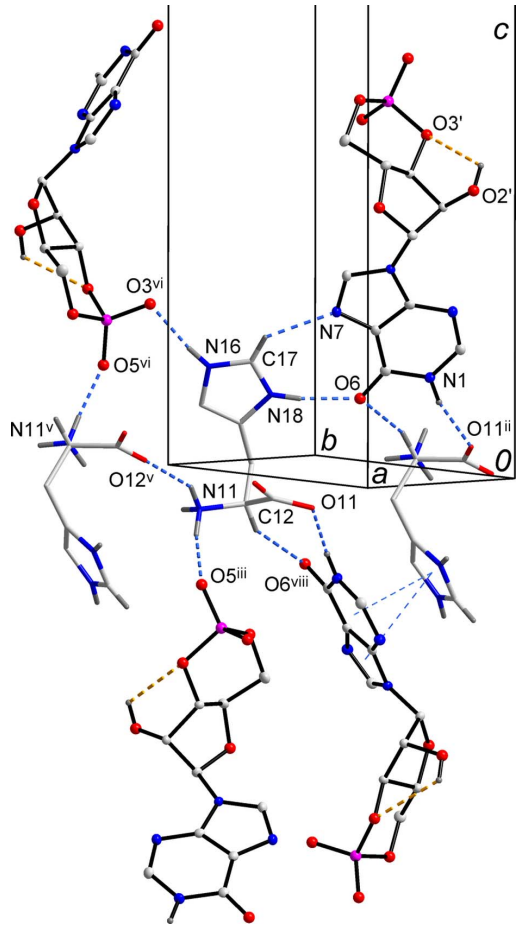

Figure 4
The complete set of His···cIMP interactions in (I). Specific and nonspecific hydrogen bonds are shown as heavy dashed lines and π–π stacking is shown as thin dashed lines. H atoms not involved in hydrogen bonds have been omitted for clarity. [Symmetry codes: (ii) $x-\frac{1}{2}$, $-y+\frac{1}{2}$, $-z+1$; (iii) $-x+\frac{3}{2}$, $-y+1$, $z-\frac{1}{2}$; (vi) $-x+2$, $y+\frac{1}{2}$, $-z+\frac{3}{2}$; (viii) $x+\frac{1}{2}$, $-y+\frac{1}{2}$, $-z+1$.]

stated that its role in nucleotide–amino acid interactions is much smaller. The phosphate group, as it has no H atom, forms only two hydrogen bonds: one of a salt-bridge type with ammonium atom N11, and the other with imidazolium atom N^{ε}16 of a different His cation (Fig. 4 and Table 2). As a result of these interactions, each cIMP anion is bound to four different His cations: to two *via* the nucleotide base and to the other two *via* the cyclic phosphate group. The fifth His cation is joined by π–π stacking of the cation···π type, as shown in Figs. 3(*b*) and 4. A similar observation is noted in His–IMP complexes. However, despite the same number of surrounding ions, the nature of these interactions is significantly different. In His–IMP complexes, as many as three of the nearest His cations are bound to the IMP anion *via* the phosphate group (two of them in a monodentate manner and the third in a bidentate manner).

In conclusion, this paper reports the preparation and solid-state structure of, and intermolecular interactions in, the first example of a 3′:5′-cyclic nucleotide–amino acid complex, namely L-His–cIMP, (I). By comparison with the analogous L-His–IMP complexes, it has been demonstrated that the 3′:5′-

cyclization of the nucleotide may reduce the nucleotide–nucleotide interactions and therefore intensify the nucleotide–amino acid interactions. In (I), both the Hoogsteen edge and the face of the Hyp base participate in specific His···cIMP recognition *via* edge-to-edge interactions and π–π stacking. The cIMP base Watson–Crick edge is involved in additional nonspecific nucleotide–amino acid contacts, which are not observed in L-His–IMP complexes. In contrast, the role of the phosphate group in nonspecific interactions is reduced compared with His–IMP complexes. This report has also focused on the cIMP conformation, against the background of the available structural information on 3′:5′-cyclic nucleotides.

Experimental

An MeOH–water solution (1:1 *v*/*v*) containing a 1:1 molar ratio of cyclic inosine 5′-phosphate sodium salt, Na(cIMP) (10 mg; Sigma) and L-histidine (L-His, 4.4 mg; ROTH) was evaporated slowly at room temperature for several days to give colourless columns of (I).

Crystal data

$C_6H_{10}N_3O_2^+\cdot C_{10}H_{10}N_4O_7P^-$
M_r = 485.36
Orthorhombic, $P2_12_12_1$
a = 5.709 (2) Å
b = 10.284 (3) Å
c = 32.795 (9) Å
V = 1925.4 (10) Å^3
Z = 4
Mo $K\alpha$ radiation
μ = 0.22 mm^{-1}
T = 90 K
0.12 × 0.07 × 0.04 mm

Data collection

Oxford Xcalibur PX κ-geometry diffractometer with an Onyx CCD camera
Absorption correction: multi-scan (*CrysAlis RED*; Oxford Diffraction, 2009)
T_{min} = 0.949, T_{max} = 1.000
17935 measured reflections
5114 independent reflections
4778 reflections with $I > 2\sigma(I)$
R_{int} = 0.032

Refinement

$R[F^2 > 2\sigma(F^2)]$ = 0.030
$wR(F^2)$ = 0.077
S = 1.04
5114 reflections
300 parameters
H-atom parameters constrained
$\Delta\rho_{max}$ = 0.35 e Å^{-3}
$\Delta\rho_{min}$ = −0.27 e Å^{-3}
Absolute structure: from known absolute configuration and anomalous dispersion effects (Flack, 1983), with 1877 Friedel pairs
Flack parameter: 0.20 (6)

All H atoms were found in difference Fourier maps. In the final refinement cycles, they were positioned geometrically and treated as riding atoms, with C—H = 0.95–1.00 Å, N—H = 0.88–0.91 Å and O—H = 0.84 Å, and with U_{iso}(H) = 1.2U_{eq}(C,Nsp^2) or 1.5U_{eq}(O,Nsp^3).

Data collection: *CrysAlis CCD* (Oxford Diffraction, 2009); cell refinement: *CrysAlis RED* (Oxford Diffraction, 2009); data reduction: *CrysAlis RED*; program(s) used to solve structure: *SHELXS97* (Sheldrick, 2008); program(s) used to refine structure: *SHELXL97* (Sheldrick, 2008); molecular graphics: *DIAMOND* (Brandenburg, 2005); software used to prepare material for publication: *SHELXL97*.

Financial support from the Faculty of Chemistry, University of Wrocław (grant No. 1494/M/WCH/11), is gratefully acknowledged.

Table 1
Selected geometric parameters (Å, °).

P1—O3	1.4968 (11)	P1—O5′	1.6060 (13)
P1—O5	1.4786 (11)	O11—C11	1.2695 (17)
P1—O3′	1.6258 (11)	O12—C11	1.2370 (19)
O3—P1—O5	117.75 (6)	O3′—P1—O5	107.58 (6)
O3—P1—O3′	108.67 (6)	O3′—P1—O5′	103.48 (6)
O3—P1—O5′	110.00 (6)	O5—P1—O5′	108.40 (6)
O3—P1—O3′—C3′	−67.24 (10)	P1—O3′—C3′—C2′	−175.96 (10)
O5—P1—O3′—C3′	164.26 (9)	P1—O5′—C5′—C4′	58.05 (14)
O5′—P1—O3′—C3′	49.65 (10)	O4′—C4′—C5′—O5′	−178.00 (11)
O3—P1—O5′—C5′	63.87 (11)	C3′—C4′—C5′—O5′	−61.29 (14)
O5—P1—O5′—C5′	−166.11 (10)	O11—C11—C12—N11	156.47 (11)
O3′—P1—O5′—C5′	−52.08 (11)	N11—C12—C13—C14	64.69 (15)
C4—N9—C1′—O4′	−174.66 (12)	C11—C12—C13—C14	−57.05 (15)
P1—O3′—C3′—C4′	−60.89 (12)	C12—C13—C14—N18	100.61 (16)

Table 2
Hydrogen-bond geometry (Å, °).

D—H···A	D—H	H···A	D···A	D—H···A
O2′—H2′···O3′	0.84	2.56	2.9671 (15)	111
O2′—H2′···O3^{i}	0.84	1.96	2.7340 (14)	154
N1—H1···O11^{ii}	0.88	1.83	2.6931 (17)	166
N11—H11A···O5^{iii}	0.91	1.79	2.6906 (16)	168
N11—H11B···O11^{iv}	0.91	1.95	2.8266 (17)	162
N11—H11B···O12^{iv}	0.91	2.52	3.2622 (19)	140
N11—H11C···O12^{v}	0.91	2.00	2.8125 (18)	148
N16—H16···O3^{vi}	0.88	1.87	2.7370 (17)	169
N18—H18···O6	0.88	1.92	2.7886 (18)	169
C2′—H2′A···O4′^{vii}	1.00	2.41	3.082 (2)	124
C3′—H3′···O2′^{iv}	1.00	2.44	3.400 (2)	160
C12—H12···O6^{viii}	1.00	2.53	3.428 (2)	149
C17—H17···N7	0.95	2.35	3.079 (2)	133

Symmetry codes: (i) $x-1, y, z$; (ii) $x-\frac{1}{2}, -y+\frac{1}{2}, -z$; (iii) $-x+\frac{3}{2}, -y+1, z-\frac{1}{2}$; (iv) $x+1, y, z$; (v) $x+\frac{1}{2}, -y+\frac{3}{2}, -z$; (vi) $-x+2, y+\frac{1}{2}, -z+\frac{1}{2}$; (vii) $-x, y-\frac{1}{2}, -z+\frac{1}{2}$; (viii) $x+\frac{1}{2}, -y+\frac{1}{2}, -z$.

Supplementary data for this paper are available from the IUCr electronic archives (Reference: QS3016). Services for accessing these data are described at the back of the journal.

References

Allen, F. H. (2002). *Acta Cryst.* B**58**, 380–388.
Bera, A. K., Mukhopadhyay, B. P., Ghosh, S., Bhattacharya, S., Chakraborty, S. & Banerjee, A. (1999). *J. Chem. Crystallogr.* **29**, 531–540.
Bernstein, J., Davis, R. E., Shimoni, L. & Chang, N.-L. (1995). *Angew. Chem. Int. Ed. Engl.* **34**, 1555–1573.
Bhattacharya, S., Bera, A. K., Ghosh, S., Chakraborty, S., Mukhopadhyay, B. P., Pal, A. & Banerjee, A. (2000). *J. Chem. Crystallogr.* **30**, 655–663.
Brandenburg, K. (2005). *DIAMOND*. Crystal Impact GbR, Bonn, Germany.
Cremer, D. & Pople, J. A. (1975). *J. Am. Chem. Soc.* **97**, 1354–1358.
Flack, H. D. (1983). *Acta Cryst.* A**39**, 876–881.
Ishida, T., Doi, M. & Inoue, M. (1988). *Nucleic Acids Res.* **16**, 6175–6190.
Ishida, T., Iyo, H., Ueda, H., Doi, M., Inoue, M., Nishimura, S. & Kitamura, K. (1991). *J. Chem. Soc. Perkin Trans. 1*, pp. 1847–1853.
Leontis, N. B. & Westhof, E. (2001). *RNA*, **7**, 499–512.
Luscombe, N. M., Laskowski, R. A. & Thornton, J. M. (2001). *Nucleic Acids Res.* **29**, 2860–2874.
Moodie, S. L. & Thornton, J. M. (1993). *Nucleic Acids Res.* **21**, 1369–1380.
Mukhopadhyay, B. P., Ghosh, S. & Banerjee, A. (1995). *J. Chem. Crystallogr.* **25**, 477–485.
Oxford Diffraction (2009). *CrysAlis CCD* and *CrysAlis RED* in Xcalibur PX software. Oxford Diffraction Ltd, Yarnton, Oxfordshire, England.
Rao, S. T., Westhof, E. & Sundaralingam, M. (1981). *Acta Cryst.* A**37**, 421–425.

Rice, P. A. & Correll, C. C. (2008). In *Protein–Nucleic Acid Interactions: Structural Biology*. Cambridge: RSC Publishing.
Sheldrick, W. S. (1983). *Z. Naturforsch. Teil B*, **38**, 982–987.
Sheldrick, G. M. (2008). *Acta Cryst.* A**64**, 112–122.
Ślepokura, K. (2008). *Carbohydr. Res.* **343**, 113–131.
Ślepokura, K. & Lis, T. (2004). *Acta Cryst.* C**60**, o315–o317.
Ślepokura, K. & Makarewicz, E. (2012). Private communication (deposition number 878282). CCDC, Union Road, Cambridge, England.
Ślepokura, K. & Mitaszewska, I. (2011). *Acta Cryst.* C**67**, o161–o165.
Ślepokura, K. & Petrus, R. (2010). *Acta Cryst.* C**66**, o265–o269.
Sundaralingam, M., Haromy, T. P. & Prusiner, P. (1982). *Acta Cryst.* B**38**, 1536–1540.

supplementary materials

Acta Cryst. (2012). C**68**, o311–o316 [doi:10.1107/S0108270112030041]

The first 3′:5′-cyclic nucleotide–amino acid complex: L-His–cIMP

Katarzyna Ślepokura

5-(2-amino-2-carboxyethyl)-1*H*-imidazol-3-ium 7-hydroxy-2-oxo-6-(6-oxo-6,9-dihydro-1*H*-purin-9-yl)-4a,6,7,7a-tetrahydro- 4*H*-1,3,5,2λ^5-furo[3,2-*d*][1,3,2λ^5]dioxaphosphinin-2-olate

Crystal data

$C_6H_{10}N_3O_2^+ \cdot C_{10}H_{10}N_4O_7P^-$
M_r = 485.36
Orthorhombic, $P2_12_12_1$
Hall symbol: P 2ac 2ab
a = 5.709 (2) Å
b = 10.284 (3) Å
c = 32.795 (9) Å
V = 1925.4 (10) Å^3
Z = 4
$F(000)$ = 1008
D_x = 1.674 Mg m^{-3}
Mo $K\alpha$ radiation, λ = 0.71073 Å
Cell parameters from 14525 reflections
θ = 2.7–38.5°
μ = 0.22 mm^{-1}
T = 90 K
Column, colourless
0.12 × 0.07 × 0.04 mm

Data collection

Oxford Xcalibur PX κ-geometry diffractometer with an Onyx CCD camera
Radiation source: Enhance (Mo) X-ray Source
Graphite monochromator
ω and φ scans
Absorption correction: multi-scan (*CrysAlis RED*; Oxford Diffraction, 2009)
T_{min} = 0.949, T_{max} = 1.000
17935 measured reflections
5114 independent reflections
4778 reflections with $I > 2\sigma(I)$
R_{int} = 0.032
θ_{max} = 30.0°, θ_{min} = 2.7°
h = −8→4
k = −12→14
l = −46→46

Refinement

Refinement on F^2
Least-squares matrix: full
$R[F^2 > 2\sigma(F^2)]$ = 0.030
$wR(F^2)$ = 0.077
S = 1.04
5114 reflections
300 parameters
0 restraints
Primary atom site location: structure-invariant direct methods
Secondary atom site location: difference Fourier map
Hydrogen site location: difference Fourier map
H-atom parameters constrained
$w = 1/[\sigma^2(F_o^2) + (0.0495P)^2 + 0.2437P]$ where $P = (F_o^2 + 2F_c^2)/3$
$(\Delta/\sigma)_{max}$ = 0.001
$\Delta\rho_{max}$ = 0.35 e Å^{-3}
$\Delta\rho_{min}$ = −0.27 e Å^{-3}
Absolute structure: from known absolute configuration and anomalous dispersion effects (Flack, 1983), with 1877 Friedel pairs
Flack parameter: 0.20 (6)

Special details

Geometry. All e.s.d.'s (except the e.s.d. in the dihedral angle between two l.s. planes) are estimated using the full covariance matrix. The cell e.s.d.'s are taken into account individually in the estimation of e.s.d.'s in distances, angles and torsion angles; correlations between e.s.d.'s in cell parameters are only used when they are defined by crystal symmetry. An approximate (isotropic) treatment of cell e.s.d.'s is used for estimating e.s.d.'s involving l.s. planes.

Refinement. Refinement of F^2 against ALL reflections. The weighted *R*-factor *wR* and goodness of fit *S* are based on F^2, conventional *R*-factors *R* are based on *F*, with *F* set to zero for negative F^2. The threshold expression of $F^2 > \sigma(F^2)$ is used only for calculating *R*-factors(gt) *etc*. and is not relevant to the choice of reflections for refinement. *R*-factors based on F^2 are statistically about twice as large as those based on *F*, and *R*-factors based on ALL data will be even larger.

Fractional atomic coordinates and isotropic or equivalent isotropic displacement parameters (Å²)

	x	*y*	*z*	U_{iso}*/U_{eq}
P1	0.38224 (6)	0.35408 (4)	0.353801 (10)	0.01193 (8)
O3	0.61881 (17)	0.31050 (12)	0.33964 (3)	0.0150 (2)
O5	0.30461 (19)	0.31239 (12)	0.39478 (3)	0.0183 (2)
O2′	−0.20278 (17)	0.35658 (12)	0.26364 (3)	0.0142 (2)
H2′	−0.2159	0.3305	0.2878	0.021*
O3′	0.18721 (17)	0.30460 (11)	0.32118 (3)	0.0116 (2)
O4′	0.16333 (18)	0.55904 (10)	0.24623 (3)	0.0130 (2)
O5′	0.36371 (19)	0.50970 (11)	0.35130 (3)	0.0160 (2)
O6	0.65016 (17)	0.29662 (11)	0.07526 (3)	0.0140 (2)
N1	0.3036 (2)	0.20214 (13)	0.09418 (3)	0.0120 (2)
H1	0.3073	0.1541	0.0720	0.014*
N3	0.0814 (2)	0.25197 (13)	0.15336 (3)	0.0129 (2)
N7	0.5859 (2)	0.46172 (13)	0.15336 (3)	0.0126 (2)
N9	0.26574 (19)	0.42739 (13)	0.19164 (3)	0.0105 (2)
C1′	0.0808 (2)	0.45442 (15)	0.22173 (4)	0.0109 (3)
H1′	−0.0663	0.4808	0.2074	0.013*
C2′	0.0302 (2)	0.33863 (15)	0.25034 (4)	0.0101 (3)
H2′A	0.0559	0.2524	0.2370	0.012*
C3′	0.2123 (2)	0.36920 (15)	0.28278 (4)	0.0099 (3)
H3′	0.3721	0.3514	0.2716	0.012*
C4′	0.1802 (2)	0.51388 (16)	0.28752 (4)	0.0117 (3)
H4′	0.0287	0.5311	0.3019	0.014*
C5′	0.3782 (3)	0.57353 (16)	0.31172 (4)	0.0146 (3)
H5′1	0.5311	0.5562	0.2986	0.018*
H5′2	0.3571	0.6687	0.3145	0.018*
C2	0.1186 (2)	0.18576 (15)	0.11985 (4)	0.0131 (3)
H2	0.0070	0.1209	0.1129	0.016*
C4	0.2533 (2)	0.34050 (15)	0.15984 (4)	0.0105 (3)
C5	0.4532 (2)	0.36319 (16)	0.13671 (4)	0.0112 (3)
C6	0.4876 (2)	0.28892 (15)	0.10027 (4)	0.0109 (3)
C8	0.4676 (2)	0.49782 (16)	0.18581 (4)	0.0125 (3)
H8	0.5167	0.5658	0.2035	0.015*
O11	0.74791 (17)	0.46360 (11)	−0.03135 (3)	0.0157 (2)
O12	0.87436 (18)	0.65877 (12)	−0.01122 (3)	0.0183 (2)
N11	1.3226 (2)	0.60432 (13)	−0.03067 (3)	0.0122 (2)
H11A	1.2980	0.6394	−0.0558	0.018*
H11B	1.4727	0.5751	−0.0289	0.018*

H11C	1.2976	0.6660	−0.0112	0.018*
N16	1.2090 (2)	0.64150 (14)	0.10327 (3)	0.0135 (2)
H16	1.2594	0.7041	0.1193	0.016*
N18	0.9928 (2)	0.48969 (13)	0.07782 (4)	0.0128 (2)
H18	0.8760	0.4350	0.0743	0.015*
C11	0.9065 (2)	0.54546 (15)	−0.02257 (4)	0.0114 (3)
C12	1.1587 (2)	0.49425 (15)	−0.02426 (4)	0.0112 (3)
H12	1.1728	0.4332	−0.0479	0.013*
C13	1.2197 (2)	0.41984 (15)	0.01512 (4)	0.0124 (3)
H13A	1.1188	0.3418	0.0171	0.015*
H13B	1.3844	0.3901	0.0136	0.015*
C14	1.1884 (2)	0.50020 (15)	0.05270 (4)	0.0114 (3)
C15	1.3233 (2)	0.59562 (16)	0.06909 (4)	0.0127 (3)
H15	1.4695	0.6254	0.0589	0.015*
C17	1.0109 (2)	0.57579 (16)	0.10796 (4)	0.0141 (3)
H17	0.9004	0.5881	0.1293	0.017*

Atomic displacement parameters (Å²)

	U^{11}	U^{22}	U^{33}	U^{12}	U^{13}	U^{23}
P1	0.00954 (14)	0.0178 (2)	0.00845 (13)	0.00116 (14)	−0.00034 (11)	−0.00065 (12)
O3	0.0097 (4)	0.0226 (7)	0.0127 (4)	0.0035 (4)	0.0010 (4)	0.0021 (4)
O5	0.0160 (5)	0.0288 (7)	0.0100 (4)	−0.0002 (5)	0.0013 (4)	−0.0004 (4)
O2′	0.0084 (4)	0.0224 (6)	0.0118 (4)	0.0001 (4)	0.0015 (3)	0.0029 (4)
O3′	0.0124 (4)	0.0138 (6)	0.0086 (4)	−0.0009 (4)	−0.0008 (3)	0.0008 (3)
O4′	0.0182 (5)	0.0096 (6)	0.0111 (4)	0.0003 (4)	0.0001 (4)	−0.0003 (3)
O5′	0.0174 (5)	0.0183 (6)	0.0124 (4)	0.0006 (4)	−0.0029 (4)	−0.0045 (4)
O6	0.0121 (4)	0.0167 (6)	0.0134 (4)	0.0007 (4)	0.0028 (3)	−0.0009 (4)
N1	0.0123 (5)	0.0113 (7)	0.0123 (5)	0.0002 (5)	0.0003 (4)	−0.0020 (4)
N3	0.0115 (5)	0.0134 (7)	0.0137 (5)	−0.0018 (4)	−0.0004 (4)	−0.0002 (4)
N7	0.0109 (5)	0.0139 (7)	0.0132 (5)	−0.0021 (4)	−0.0002 (4)	0.0001 (4)
N9	0.0093 (5)	0.0125 (7)	0.0096 (4)	−0.0008 (4)	0.0006 (4)	0.0006 (4)
C1′	0.0096 (6)	0.0129 (8)	0.0103 (5)	0.0010 (5)	0.0013 (4)	−0.0011 (4)
C2′	0.0080 (5)	0.0126 (8)	0.0096 (5)	−0.0008 (5)	0.0001 (4)	0.0004 (5)
C3′	0.0090 (5)	0.0125 (8)	0.0083 (5)	0.0001 (5)	−0.0003 (4)	0.0006 (4)
C4′	0.0117 (6)	0.0133 (8)	0.0101 (5)	0.0005 (5)	−0.0008 (4)	−0.0012 (5)
C5′	0.0151 (6)	0.0130 (8)	0.0157 (6)	−0.0015 (6)	−0.0019 (5)	−0.0024 (5)
C2	0.0126 (6)	0.0120 (8)	0.0146 (5)	−0.0009 (5)	0.0000 (5)	0.0009 (5)
C4	0.0108 (5)	0.0110 (8)	0.0097 (5)	0.0016 (5)	−0.0003 (4)	0.0018 (4)
C5	0.0098 (5)	0.0132 (8)	0.0107 (5)	0.0003 (5)	−0.0009 (4)	0.0022 (5)
C6	0.0113 (6)	0.0098 (8)	0.0116 (5)	0.0025 (5)	−0.0009 (4)	0.0021 (5)
C8	0.0104 (5)	0.0138 (8)	0.0132 (6)	−0.0021 (5)	−0.0012 (5)	0.0005 (5)
O11	0.0106 (4)	0.0189 (7)	0.0175 (5)	0.0000 (4)	−0.0010 (4)	−0.0040 (4)
O12	0.0151 (5)	0.0155 (7)	0.0244 (5)	0.0054 (4)	−0.0016 (4)	−0.0069 (4)
N11	0.0099 (5)	0.0159 (7)	0.0107 (5)	0.0003 (4)	−0.0003 (4)	−0.0013 (4)
N16	0.0141 (5)	0.0153 (7)	0.0112 (5)	−0.0013 (5)	−0.0010 (4)	−0.0005 (4)
N18	0.0100 (5)	0.0144 (7)	0.0141 (5)	−0.0011 (5)	−0.0006 (4)	0.0016 (4)
C11	0.0107 (5)	0.0148 (8)	0.0087 (5)	0.0024 (5)	−0.0016 (4)	−0.0010 (4)
C12	0.0102 (5)	0.0117 (8)	0.0118 (5)	0.0008 (5)	−0.0017 (4)	−0.0023 (5)
C13	0.0134 (6)	0.0101 (8)	0.0138 (5)	0.0018 (5)	−0.0022 (5)	−0.0005 (5)

C14	0.0097 (5)	0.0129 (8)	0.0116 (5)	0.0000 (5)	−0.0010 (4)	0.0026 (5)
C15	0.0120 (6)	0.0152 (8)	0.0111 (5)	−0.0010 (5)	−0.0003 (5)	0.0021 (5)
C17	0.0131 (6)	0.0172 (9)	0.0122 (5)	0.0015 (6)	0.0008 (5)	0.0019 (5)

Geometric parameters (Å, º)

P1—O3	1.4968 (11)	C4′—H4′	1.00
P1—O5	1.4786 (11)	C5′—H5′1	0.99
P1—O3′	1.6258 (11)	C5′—H5′2	0.99
P1—O5′	1.6060 (13)	C2—H2	0.95
O2′—C2′	1.4117 (16)	C4—C5	1.3903 (18)
O2′—H2′	0.84	C5—C6	1.4318 (19)
O3′—C3′	1.4309 (15)	C8—H8	0.95
O4′—C1′	1.4232 (17)	O11—C11	1.2695 (17)
O4′—C4′	1.4348 (16)	O12—C11	1.2370 (19)
O5′—C5′	1.4568 (17)	N11—C12	1.4837 (19)
O6—C6	1.2412 (17)	N11—H11A	0.91
N1—C2	1.3613 (18)	N11—H11B	0.91
N1—C6	1.392 (2)	N11—H11C	0.91
N1—H1	0.88	N16—C17	1.3266 (19)
N3—C2	1.3100 (18)	N16—C15	1.3798 (17)
N3—C4	1.3555 (19)	N16—H16	0.88
N7—C8	1.3138 (18)	N18—C17	1.3312 (19)
N7—C5	1.3777 (19)	N18—C14	1.3918 (17)
N9—C8	1.3746 (18)	N18—H18	0.88
N9—C4	1.3750 (18)	C11—C12	1.5339 (19)
N9—C1′	1.4716 (17)	C12—C13	1.5409 (19)
C1′—C2′	1.544 (2)	C12—H12	1.00
C1′—H1′	1.00	C13—C14	1.4945 (19)
C2′—C3′	1.5204 (18)	C13—H13A	0.99
C2′—H2′A	1.00	C13—H13B	0.99
C3′—C4′	1.507 (2)	C14—C15	1.358 (2)
C3′—H3′	1.00	C15—H15	0.95
C4′—C5′	1.511 (2)	C17—H17	0.95
O3—P1—O5	117.75 (6)	N1—C2—H2	117.3
O3—P1—O3′	108.67 (6)	N3—C4—N9	126.36 (12)
O3—P1—O5′	110.00 (6)	N3—C4—C5	128.42 (13)
O3′—P1—O5	107.58 (6)	N9—C4—C5	105.21 (12)
O3′—P1—O5′	103.48 (6)	N7—C5—C4	111.00 (12)
O5—P1—O5′	108.40 (6)	N7—C5—C6	130.39 (12)
C2′—O2′—H2′	109.5	C4—C5—C6	118.58 (13)
C3′—O3′—P1	111.42 (8)	O6—C6—N1	120.68 (13)
C1′—O4′—C4′	108.09 (11)	O6—C6—C5	128.30 (14)
C5′—O5′—P1	119.39 (9)	N1—C6—C5	111.00 (12)
C2—N1—C6	125.17 (12)	N7—C8—N9	113.24 (13)
C2—N1—H1	117.4	N7—C8—H8	123.4
C6—N1—H1	117.4	N9—C8—H8	123.4
C2—N3—C4	111.32 (12)	C12—N11—H11A	109.5
C8—N7—C5	104.27 (12)	C12—N11—H11B	109.5

C8—N9—C4	106.28 (11)	H11A—N11—H11B	109.5
C8—N9—C1′	126.53 (12)	C12—N11—H11C	109.5
C4—N9—C1′	126.45 (11)	H11A—N11—H11C	109.5
O4′—C1′—N9	106.50 (11)	H11B—N11—H11C	109.5
O4′—C1′—C2′	107.57 (10)	C17—N16—C15	108.84 (13)
N9—C1′—C2′	113.35 (12)	C17—N16—H16	125.6
O4′—C1′—H1′	109.8	C15—N16—H16	125.6
N9—C1′—H1′	109.8	C17—N18—C14	109.00 (12)
C2′—C1′—H1′	109.8	C17—N18—H18	125.5
O2′—C2′—C3′	113.65 (10)	C14—N18—H18	125.5
O2′—C2′—C1′	105.27 (11)	O12—C11—O11	125.94 (13)
C3′—C2′—C1′	97.92 (11)	O12—C11—C12	118.28 (12)
O2′—C2′—H2′A	112.9	O11—C11—C12	115.70 (13)
C3′—C2′—H2′A	112.9	N11—C12—C11	109.58 (12)
C1′—C2′—H2′A	112.9	N11—C12—C13	110.80 (11)
O3′—C3′—C4′	110.82 (10)	C11—C12—C13	110.62 (11)
O3′—C3′—C2′	116.82 (11)	N11—C12—H12	108.6
C4′—C3′—C2′	101.13 (11)	C11—C12—H12	108.6
O3′—C3′—H3′	109.2	C13—C12—H12	108.6
C4′—C3′—H3′	109.2	C14—C13—C12	112.93 (12)
C2′—C3′—H3′	109.2	C14—C13—H13A	109.0
O4′—C4′—C3′	103.32 (10)	C12—C13—H13A	109.0
O4′—C4′—C5′	114.48 (12)	C14—C13—H13B	109.0
C3′—C4′—C5′	111.33 (12)	C12—C13—H13B	109.0
O4′—C4′—H4′	109.2	H13A—C13—H13B	107.8
C3′—C4′—H4′	109.2	C15—C14—N18	106.06 (12)
C5′—C4′—H4′	109.2	C15—C14—C13	131.17 (13)
O5′—C5′—C4′	104.02 (12)	N18—C14—C13	122.74 (13)
O5′—C5′—H5′1	111.0	C14—C15—N16	107.50 (12)
C4′—C5′—H5′1	111.0	C14—C15—H15	126.2
O5′—C5′—H5′2	111.0	N16—C15—H15	126.2
C4′—C5′—H5′2	111.0	N16—C17—N18	108.59 (12)
H5′1—C5′—H5′2	109.0	N16—C17—H17	125.7
N3—C2—N1	125.45 (14)	N18—C17—H17	125.7
N3—C2—H2	117.3		

O3—P1—O3′—C3′	−67.24 (10)	C8—N9—C4—N3	−179.69 (14)
O5—P1—O3′—C3′	164.26 (9)	C1′—N9—C4—N3	−9.1 (2)
O5′—P1—O3′—C3′	49.65 (10)	C8—N9—C4—C5	0.73 (15)
O3—P1—O5′—C5′	63.87 (11)	C1′—N9—C4—C5	171.35 (13)
O5—P1—O5′—C5′	−166.11 (10)	C8—N7—C5—C4	−0.18 (16)
O3′—P1—O5′—C5′	−52.08 (11)	C8—N7—C5—C6	177.46 (15)
C4′—O4′—C1′—N9	−118.53 (11)	N3—C4—C5—N7	−179.93 (14)
C4′—O4′—C1′—C2′	3.29 (13)	N9—C4—C5—N7	−0.36 (16)
C8—N9—C1′—O4′	−5.89 (18)	N3—C4—C5—C6	2.1 (2)
C4—N9—C1′—O4′	−174.66 (12)	N9—C4—C5—C6	−178.31 (12)
C8—N9—C1′—C2′	−123.97 (14)	C2—N1—C6—O6	179.53 (13)
C4—N9—C1′—C2′	67.26 (17)	C2—N1—C6—C5	−2.06 (19)
O4′—C1′—C2′—O2′	87.45 (12)	N7—C5—C6—O6	0.8 (3)

N9—C1′—C2′—O2′	−155.09 (10)	C4—C5—C6—O6	178.25 (14)
O4′—C1′—C2′—C3′	−29.79 (12)	N7—C5—C6—N1	−177.49 (14)
N9—C1′—C2′—C3′	87.66 (12)	C4—C5—C6—N1	0.00 (18)
P1—O3′—C3′—C4′	−60.89 (12)	C5—N7—C8—N9	0.68 (16)
P1—O3′—C3′—C2′	−175.96 (10)	C4—N9—C8—N7	−0.92 (16)
O2′—C2′—C3′—O3′	53.48 (17)	C1′—N9—C8—N7	−171.53 (13)
C1′—C2′—C3′—O3′	164.04 (11)	O12—C11—C12—N11	−26.71 (16)
O2′—C2′—C3′—C4′	−66.87 (14)	O11—C11—C12—N11	156.47 (11)
C1′—C2′—C3′—C4′	43.69 (11)	O12—C11—C12—C13	95.75 (15)
C1′—O4′—C4′—C3′	25.38 (13)	O11—C11—C12—C13	−81.08 (15)
C1′—O4′—C4′—C5′	146.61 (12)	N11—C12—C13—C14	64.69 (15)
O3′—C3′—C4′—O4′	−168.80 (10)	C11—C12—C13—C14	−57.05 (15)
C2′—C3′—C4′—O4′	−44.26 (12)	C17—N18—C14—C15	0.05 (16)
O3′—C3′—C4′—C5′	67.87 (14)	C17—N18—C14—C13	−178.10 (13)
C2′—C3′—C4′—C5′	−167.60 (11)	C12—C13—C14—C15	−77.04 (19)
P1—O5′—C5′—C4′	58.05 (14)	C12—C13—C14—N18	100.61 (16)
O4′—C4′—C5′—O5′	−178.00 (11)	N18—C14—C15—N16	−0.29 (16)
C3′—C4′—C5′—O5′	−61.29 (14)	C13—C14—C15—N16	177.65 (14)
C4—N3—C2—N1	−0.3 (2)	C17—N16—C15—C14	0.43 (16)
C6—N1—C2—N3	2.4 (2)	C15—N16—C17—N18	−0.40 (16)
C2—N3—C4—N9	178.59 (14)	C14—N18—C17—N16	0.22 (16)
C2—N3—C4—C5	−1.9 (2)		

Hydrogen-bond geometry (Å, º)

D—H···*A*	*D*—H	H···*A*	*D*···*A*	*D*—H···*A*
O2′—H2′···O3′	0.84	2.56	2.9671 (15)	111
O2′—H2′···O3^{i}	0.84	1.96	2.7340 (14)	154
N1—H1···O11^{ii}	0.88	1.83	2.6931 (17)	166
N11—H11*A*···O5^{iii}	0.91	1.79	2.6906 (16)	168
N11—H11*B*···O11^{iv}	0.91	1.95	2.8266 (17)	162
N11—H11*B*···O12^{iv}	0.91	2.52	3.2622 (19)	140
N11—H11*C*···O12^{v}	0.91	2.00	2.8125 (18)	148
N16—H16···O3^{vi}	0.88	1.87	2.7370 (17)	169
N18—H18···O6	0.88	1.92	2.7886 (18)	169
C2′—H2′*A*···O4′^{vii}	1.00	2.41	3.082 (2)	124
C3′—H3′···O2′^{iv}	1.00	2.44	3.400 (2)	160
C12—H12···O6^{viii}	1.00	2.53	3.428 (2)	149
C17—H17···N7	0.95	2.35	3.079 (2)	133

Symmetry codes: (i) *x*−1, *y*, *z*; (ii) *x*−1/2, −*y*+1/2, −*z*; (iii) −*x*+3/2, −*y*+1, *z*−1/2; (iv) *x*+1, *y*, *z*; (v) *x*+1/2, −*y*+3/2, −*z*; (vi) −*x*+2, *y*+1/2, −*z*+1/2; (vii) −*x*, *y*−1/2, −*z*+1/2; (viii) *x*+1/2, −*y*+1/2, −*z*.